On the Performance of Wireless Energy Harvesting Networks in a Boolean-Poisson Model

Han-Bae Kong†, Ian Flint‡, Dusit Niyato†, and Nicolas Privault‡
†School of Computer Engineering, Nanyang Technological University, Singapore
‡School of Physical and Mathematical Sciences, Nanyang Technological University, Singapore

***Abstract*—Wireless radio frequency (RF) energy harvesting has been adopted in wireless networks as a method to supply energy to wireless nodes, e.g., sensors. In this paper, we present a new analysis of the wireless energy harvesting network based on a Boolean-Poisson model. This model considers that the energy sources have a fixed coverage range. The energy sources are distributed according to a Poisson point process (PPP) while their radii of coverage are random and are assumed to follow a given probability distribution. We derive the performance measures consisting of the energy harvesting probability and the transmission success probability both in the cases of two nodes and multiple nodes. Our analysis is validated by simulation.**

***Index Terms*—RF energy harvesting, Boolean-Poisson model, multihop networks.**

I. Introduction

Recently, RF energy harvesting techniques have been developed to let mobile and sensor nodes scavenge energy from radiated RF signals from ambient or dedicated RF sources [1]. Due to its advantages of powering energy-constrained devices and prolonging the lifetime of wireless networks, many researchers have studied energy harvesting methods in various wireless network scenarios [2]–[7]. For example, in [2]–[4], transmit beamforming methods which optimize the performance were developed for the networks where energy harvesting nodes collect power from the RF signals sent by its dedicated RF energy transmitters. To analyze the performance of the network with RF energy harvesting capability, analytical models based on a Poisson point process (PPP) were introduced [5]–[7]. In such models, the locations of RF energy sources are geographically distributed according to the PPP, assuming that nodes in the networks harvest energy from the signals transmitted by surrounding energy sources. The study in [5] introduced a tradeoff among transmit power, density of base stations, and density of energy sources in an uplink cellular network. In [6], the authors derived the outage probability of a network overlaid with power beacons distributed according to a PPP. Alternatively, the authors in [7] investigated the transmission success probability in an RF energy harvesting multi-tier uplink cellular network by modeling the level of stored energy as a Markov chain.

In wireless energy harvesting networks, one can consider the coverage region of an RF energy source, i.e. an energy harvesting enabled area formed by the RF signals from the energy source. Then, the union of the coverage regions can be understood as the energy harvesting enabled region in the networks. In this sense, the probability that nodes can harvest energy is related to not only the distribution of the locations of the RF energy sources, but also characteristics of the coverage region. However, most previous works on energy harvesting networks have not taken the features of the coverage regions into account when analyzing the networks.

In this paper, we assume that the RF energy sources are distributed according to a homogeneous PPP, and the coverage region of a RF source is a disc of random radius. This model is known in the literature as the Boolean model. The Boolean model has been extensively studied, cf. [8] and [9] for a thorough overview, and the coverage properties of the model were investigated in [10]–[12]. The model has been used in different applications, see [8]. More specific examples are [13] for applications to image analysis and [14], [15] for applications to wireless networks. However, its application to wireless energy harvesting networks has not been previously considered.

The analysis presented in this paper considers two major situations arising in RF energy harvesting networks, i.e., two node harvesting and multiple node harvesting. The performance measures in terms of the energy harvesting probability and transmission success probability are derived. As for the mathematical contributions, Theorem 1 provides the probability that two nodes at fixed locations are covered by the Boolean model. This is the situation in which the nodes can harvest energy and are able to communicate with each other. We extend the computation of Theorem 1 to the case of multiple nodes at aligned fixed points. These nodes are part of a multihop link, and thus the important performance metric is an end-to-end transmission success probability. We find that these results depend only on the law of the radius, and we provide some explicit computations for a panel of common distributions.

II. The Boolean-Poisson model

This section introduces the required background for the study of the Boolean-Poisson model which is also known as a Boolean model. Let us define μ a probability measure on $[0,\infty)$ and consider the probability space $(\Omega,\mathcal{F},\mathbb{P})$ on which we let Φ be a PPP supported on $\mathbb{R}^d\times[0,\infty)$. The intensity measure is $\ell\otimes(\lambda\mu)$, where ℓ indicates the Lebesgue measure on $\mathbb{R}^d$. We denote by $\mathcal{B}_x(r)$ the open Euclidean ball of $\mathbb{R}^d$ centered at $x\in\mathbb{R}^d$ with radius $r\in[0,\infty)$. Moreover, we consider the following random set

$$\Xi=\bigcup_{(x,r)\in\Phi}\mathcal{B}_x(r), \tag{1}$$

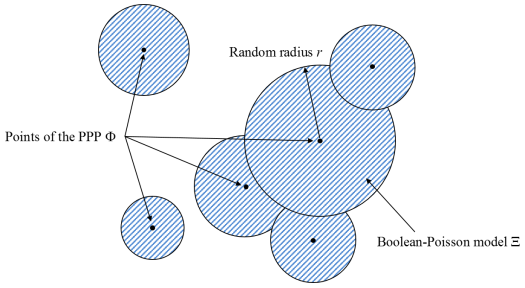

Fig. 1: Description of the Boolean-Poisson model

which consists of all points covered by at least one ball. The set Ξ is called the Boolean-Poisson model, and Φ is the underlying PPP containing the pairs (x, r) of points along with their corresponding radius. We illustrate the model in Fig. 1.

In the Boolean-Poisson model, the metric of interest is the probability that a fixed point in $\mathbb{R}^d$ is covered by the union of balls. Let us consider a point A in space located at $x \in \mathbb{R}^d$ and define the set

$$\mathcal{C}_x = \left\{ (y, r) \in \mathbb{R}^d \times [0, \infty) : y \in \mathcal{B}_x(r) \right\}. \tag{2}$$

Then, since $x \notin \Xi \iff \Phi \cap \mathcal{C}_x = \emptyset$, the probability that the point A falls in Ξ can be computed by fairly standard calculations:

$$\begin{aligned} \mathbb{P}(x \in \Xi) &= 1 - \mathbb{P}(\Phi \cap \mathcal{C}_x = \emptyset) \\ &= 1 - \exp\left(-(\ell \otimes (\lambda\mu))(\mathcal{C}_x)\right) \\ &= 1 - \exp\left(-\lambda \int_0^\infty \ell(\mathcal{B}_x(r))\, \mu(\mathrm{d}r)\right) \\ &= 1 - \exp\left(-\lambda v_d \int_0^\infty r^d\, \mu(\mathrm{d}r)\right), \end{aligned} \tag{3}$$

where $v_d \triangleq \pi^{d/2}/\Gamma(d/2+1)$ represents the volume of the d-dimensional Euclidean ball, and $\Gamma(\cdot)$ is the Gamma function. Note that $\mathbb{P}(x \in \Xi) = 1$ when $\int_0^\infty r^d \mu(\mathrm{d}r) = \infty$. Therefore, we can infer that a point in $\mathbb{R}^d$ is almost surely covered by the Boolean-Poisson model if the d-th moment of μ is infinite.

III. System Model

In this paper, we analyze the wireless energy harvesting networks consisting of a (random) number of ambient RF energy sources. In the networks, sensor nodes harvest energy from the RF signals radiated by the ambient RF energy sources, and transmit or receive data by using the harvested energy. The homogeneous PPP Φ with density λ models the locations of the ambient RF energy sources. Also, we assume that each energy source has its own coverage region, and the sensor nodes in the region can scavenge energy from one of the energy sources. The coverage region of each ambient RF energy source is modeled by the open Euclidean ball of $\mathbb{R}^d$ centered at the location of the energy source with a randomly distributed radius distributed according to μ. By construction, the energy harvesting enabled region is modeled as the Boolean-Poisson model Ξ as defined in (1). Fig. 2 illustrates a realization of the network where $d = 2$, $\lambda = 0.04$, and the radius is exponentially distributed, i.e., $\mu(\mathrm{d}r) = \rho \exp(-\rho r)\, \mathrm{d}r$ with $\rho = 0.5$.

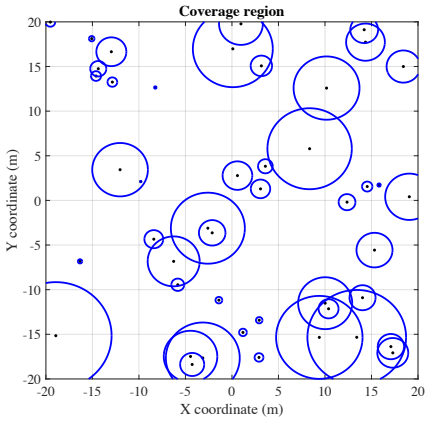

Fig. 2: A realization of the network in a Boolean-Poisson model where black dots and blue circles represent the locations of the ambient RF energy sources and boundaries of the coverage region

It is worthwhile to note that exploiting the Boolean-Poisson model to model the energy harvesting networks is a new approach and different from the conventional approach in [5]–[7]. Most previous works on the wireless energy harvesting networks have not considered characteristics of the coverage range and only focused on the locations of the energy sources. However, the probability that a sensor node in the network can harvest energy is strongly dependent on the distribution of the coverage range. Therefore, it is important to investigate the performance of the networks where the energy harvesting enabled region is modeled as the Boolean-Poisson model.

Let us consider n sensor nodes $\mathrm{A}_1, \mathrm{A}_2, \ldots, \mathrm{A}_n$ which are respectively located at $x_1 \in \mathbb{R}^d, x_2 \in \mathbb{R}^d, \ldots, x_n \in \mathbb{R}^d$. We assume multi-hop networks where node A_1 transmits data to node A_n aided by nodes $\mathrm{A}_2, \ldots, \mathrm{A}_{n-1}$. In this case, the transmission succeeds when all nodes are located in the energy harvesting enabled region Ξ, and the received signal-to-noise-ratio (SNR) of each hop is larger than a certain threshold γ_{th} which means the minimum SNR required for the successful data detection. Therefore, by defining P_H and P_T as the probabilities that all nodes can harvest energy and the received SNRs for all hops are higher than γ_{th}, respectively, the transmission success probability P_S can be expressed as

$$P_S = P_H P_T, \tag{4}$$

where

$$P_H = \mathbb{P}(\forall k \in \{1, \ldots, n\},\ x_k \in \Xi), \tag{5}$$

and

$$P_T = \mathbb{P}(\forall k \in \{1, \ldots, n-1\}, \gamma_k \geq \gamma_{th}). \tag{6}$$

Here, $\gamma_k \triangleq \frac{P h_k ||x_{k+1} - x_k||^{-\alpha}}{\sigma^2}$ stands for the received SNR for the k-th hop where P is the transmit power at all nodes, h_k denotes the fading power for the k-th hop, α indicates the pathloss exponent, and σ^2 accounts for the power of additive white Gaussian noise. In this paper, the fading powers

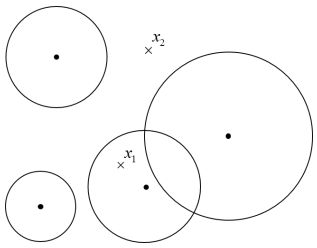

(a) Non-coverage: only A_1 is covered

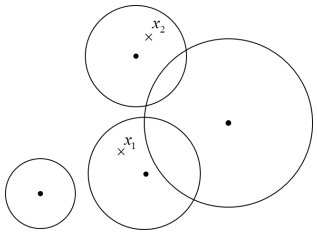

(b) Coverage: both A_1 and A_2 are covered

Fig. 3: Examples to illustrate networks with two nodes

$\{h_k\}$ are assumed to follow independently and identically distributed (i.i.d.) exponential distribution with parameter τ. It is also assumed that the $\{h_k\}$ are independent of the PPP Φ.

IV. Performance Analysis

In this section, we first derive an analytical expression for the transmission success probability in the networks where two nodes exist. Then, we generalize the analytical result to the case of the networks with multiple nodes.

A. Networks with two nodes

Let us consider two nodes A_1 and A_2 which are located at $x_1 \in \mathbb{R}^d$ and $x_2 \in \mathbb{R}^d$, respectively. Note that both A_1 and A_2 ought to be located in Ξ in order to scavenge energy. As an illustration, the placement of A_2 in Fig. 3a corresponds to a non-coverage situation, whereas that of in Fig. 3b corresponds to a coverage situation.

In the networks with two nodes, the coverage probability P_H in (5) can be rewritten as

$$\begin{aligned} P_H &= \mathbb{P}\left(x_1 \in \Xi\right) + \mathbb{P}\left(x_2 \in \Xi\right) - \mathbb{P}\left(\{x_1 \in \Xi\} \cup \{x_2 \in \Xi\}\right) \\ &\overset{\text{(a)}}{=} 2 - 2\exp\left(-\lambda v_d \int_0^\infty r^d \,\mu(\mathrm{d}r)\right) \\ &\qquad - \mathbb{P}\left(\{x_1 \in \Xi\} \cup \{x_2 \in \Xi\}\right), \end{aligned} \tag{7}$$

where (a) follows from the result in (3) and the stationarity of the PPP. In the following theorem, we provide an analytical expression for P_H.

Theorem 1: In the networks with two nodes, the probability that both nodes can harvest energy is given by

$$\begin{aligned} P_H &= 1 - 2\exp\left(-\lambda v_d \int_0^\infty r^d \,\mu(\mathrm{d}r)\right) \\ &\quad + \exp\left(-2\lambda v_d \int_0^\infty r^d \,\mu(\mathrm{d}r)\right. \\ &\quad \left. + \lambda v_d \int_{l/2}^\infty I_{1-l^2/(4r^2)}\left(\frac{d+1}{2}, \frac{1}{2}\right) r^d \,\mu(\mathrm{d}r)\right), \end{aligned} \tag{8}$$

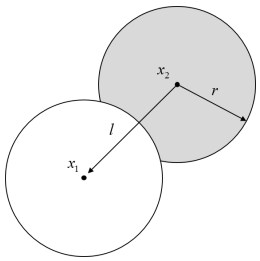

Fig. 4: An illustration for the case of $r \geq l/2$

where $l \triangleq \|x_1 - x_2\|$ is the distance between A_1 and A_2. Here, $I_z(a,b)$ is the regularized incomplete beta function defined by

$$I_z(a,b) = \frac{\Gamma(a+b)\int_0^z u^{a-1}(1-u)^{b-1}\,\mathrm{d}u}{\Gamma(a)\Gamma(b)}, \quad a,b,z > 0.$$

Proof: Let us define Φ_{x_1} as a PPP on the same probability space as Φ, supported on $\mathcal{C}_{x_1}^c$ with intensity measure $\ell \otimes (\lambda\mu)$ restricted to $\mathcal{C}_{x_1}^c$, where X^c denotes the complement of a set X. Recall that $\mathcal{C}_{x_1}$ has been defined in (2). We define accordingly the Boolean-Poisson model associated to Φ_{x_1} as $\Xi_{x_1} = \bigcup_{(x,r)\in\Phi_{x_1}} \mathcal{B}_x(r)$. Then, we have

$$\begin{aligned} \mathbb{P}\left(x_2 \notin \Xi_{x_1}\right) &= \mathbb{P}\left(\{(y,r) \in \Phi_{x_1} : x_2 \in \mathcal{B}_y(r)\} = \emptyset\right) \\ &= \mathbb{P}\left(\Phi_{x_1} \cap \mathcal{C}_{x_2} = \emptyset\right) \\ &= \exp\left(-(\ell \otimes (\lambda\mu))\left(\mathcal{C}_{x_2} \cap \mathcal{C}_{x_1}^c\right)\right) \\ &= \exp\left(-\lambda \int_0^\infty \ell\left(\mathcal{B}_{x_2}(r) \cap \mathcal{B}_{x_1}(r)^c\right)\mu(\mathrm{d}r)\right). \end{aligned}$$

Now, we focus on the computation of the volume in the above equation. First, if $r < l/2$, then $\ell\left(\mathcal{B}_{x_2}(r) \cap \mathcal{B}_{x_1}(r)^c\right) = \ell\left(\mathcal{B}_{x_2}(r)\right) = v_d r^d$. Second, if $r \geq l/2$, then one has to compute the shaded area in Fig. 4 (represented here in dimension $d = 2$). The above d-dimensional volume (known in the literature as hyperspherical cap) is equal to [16]

$$\ell\left(\mathcal{B}_{x_2}(r) \cap \mathcal{B}_{x_1}(r)^c\right) = v_d r^d \left(1 - I_{1-l^2/(4r^2)}\left(\frac{d+1}{2}, \frac{1}{2}\right)\right).$$

Hence, $\mathbb{P}\left(x_2 \notin \Xi_{x_1}\right)$ becomes

$$\begin{aligned} \mathbb{P}\left(x_2 \notin \Xi_{x_1}\right) &= \exp\left(-\lambda v_d \int_0^\infty r^d \,\mu(\mathrm{d}r)\right. \\ &\quad \left. + \lambda v_d \int_{l/2}^\infty I_{1-l^2/(4r^2)}\left(\frac{d+1}{2}, \frac{1}{2}\right) r^d \,\mu(\mathrm{d}r)\right). \end{aligned} \tag{9}$$

Note that the law of Φ given $\Phi \cap \mathcal{C}_{x_1} = \emptyset$ coincides with the distribution of Φ_{x_1}, and therefore $\mathbb{P}\left(\{x_1 \in \Xi\} \cup \{x_2 \in \Xi\}\right)$ in (7) can be written as

$$\begin{aligned} &\mathbb{P}\left(\{x_1 \in \Xi\} \cup \{x_2 \in \Xi\}\right) \\ &\quad = 1 - \mathbb{P}\left(x_1 \notin \Xi\right)\mathbb{P}\left(x_2 \notin \Xi \mid x_1 \notin \Xi\right) \\ &\quad = 1 - \mathbb{P}\left(x_1 \notin \Xi\right)\mathbb{P}\left(x_2 \notin \Xi \mid \Phi \cap \mathcal{C}_{x_1} = \emptyset\right) \\ &\quad = 1 - \mathbb{P}\left(x_1 \notin \Xi\right)\mathbb{P}\left(x_2 \notin \Xi_{x_1}\right). \end{aligned} \tag{10}$$

Combining (7), (9) and (10), we obtain the result in (8). ■

In the following corollary, we customize Theorem 1 to the case $d = 2$, which is the main situation of interest.

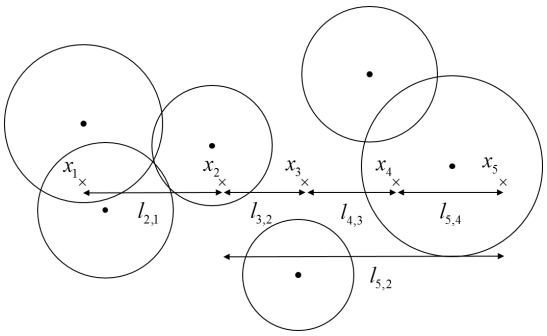

Fig. 5: An example to illustrate networks with multiple nodes

Corollary 1: When $d = 2$, the coverage probability can be simplified as

$$P_H = 1 - 2\exp\left(-\lambda\pi\int_0^\infty r^2\,\mu(\mathrm{d}r)\right) + \exp\left(-2\lambda\pi\int_0^\infty r^2\,\mu(\mathrm{d}r) + 2\lambda\int_{l/2}^\infty \left(\arccos\left(\frac{l}{2r}\right) - \frac{l}{2r}\sqrt{1-\frac{l^2}{4r^2}}\right) r^2\,\mu(\mathrm{d}r)\right), \tag{11}$$

where $\arccos(\cdot)$ denotes the inverse cosine function, and we recall that l is the distance between A_1 and A_2.

Proof: By using mathematical software such as Mathematica, we may rewrite $I_{1-l^2/(4r^2)}\left(\frac{3}{2},\frac{1}{2}\right)$ as

$$I_{1-l^2/(4r^2)}\left(\frac{3}{2},\frac{1}{2}\right) = \frac{2}{\pi}\int_0^{1-l^2/(4r^2)} \sqrt{\frac{u}{1-u}}\,\mathrm{d}u = \frac{2}{\pi}\left(\arccos\left(\frac{l}{2r}\right) - \frac{l}{2r}\sqrt{1-\frac{l^2}{4r^2}}\right).$$

Also, if $d = 2$, v_2 is equal to π. From these results, we derive the expression in (11). ∎

When the networks consists of only two nodes, P_T in (6) is easily computed as

$$P_T = \mathbb{P}\left(\frac{Ph_1 l^{-\alpha}}{\sigma^2} \geq \gamma_{th}\right) = \exp\left(-\frac{\tau l^\alpha \sigma^2 \gamma_{th}}{P}\right). \tag{12}$$

From (8), (11) and (12), we deduce the transmission success probability in (4).

B. Networks with multiple nodes

In this subsection, we concentrate on the wireless energy harvesting networks containing multiple nodes. Let us consider $\mathrm{A}_1, \ldots, \mathrm{A}_n$ nodes (here $n \geq 2$) which are located at $x_1 \in \mathbb{R}^d, \ldots, x_n \in \mathbb{R}^d$, respectively, and define the inter-nodal distance as

$$l_{a,b} \triangleq \|x_b - x_a\|, \quad a, b \in \{1, \ldots, n\}.$$

We assume that the nodes are aligned as shown in Fig. 5. In this example, as node A_3 is not covered, node A_3 does not have available power for data decoding and encoding, and therefore outage occurs when node A_1 attempts to communicate with node A_5 through nodes A_2, A_3 and A_4.

We remark that P_H can be computed as

$$\begin{aligned}&\mathbb{P}\left(\forall k \in \{1,\ldots,n\},\ x_k \in \Xi\right)\\ &= 1 - \mathbb{P}\left(\exists k \in \{1,\ldots,n\},\ x_k \notin \Xi\right)\\ &\overset{\text{(c)}}{=} 1 + \sum_{X\subset\{1,\ldots,n\},\ X\neq\emptyset} (-1)^{|X|}\mathbb{P}\left(\forall k \in X,\ x_k \notin \Xi\right),\end{aligned} \tag{13}$$

where (c) follows from the inclusion-exclusion principle and $|X|$ denotes the cardinal of a set X.

We exploit relation (13) in the following theorem, wherein we derive a procedure for computing the probability that all n nodes are covered by the Boolean-Poisson model.

Theorem 2: Let $X = (a_1, \ldots, a_n) \subset \{1, \ldots, n\}$ correspond to one of the terms appearing in (13). Then $\mathbb{P}\left(\forall k \in X,\ x_k \notin \Xi\right)$ is given inductively by

$$\begin{aligned}&\mathbb{P}\left(\forall k \in \{a_1,\ldots,a_n\},\ x_k \notin \Xi\right)\\ &= \mathbb{P}\left(\forall k \in \{a_1,\ldots,a_{n-1}\},\ x_k \notin \Xi\right)\\ &\times \exp\left(-\lambda v_d \int_0^\infty r^d\,\mu(\mathrm{d}r)\right.\\ &\left.+\lambda v_d \int_{\frac{l_{a_n,a_{n-1}}}{2}}^\infty I_{1-\frac{l^2_{a_n,a_{n-1}}}{4r^2}}\left(\frac{d+1}{2},\frac{1}{2}\right) r^d\,\mu(\mathrm{d}r)\right),\end{aligned}$$

whilst noting that the initial term $\mathbb{P}\left(x_{a_1} \notin \Xi,\ x_{a_2} \notin \Xi\right)$ has been computed in Theorem 1.

Proof: In this setting, one may compute the probability in the summation in (13) by induction as follows:

$$\begin{aligned}&\mathbb{P}\left(\forall k \in \{a_1,\ldots,a_n\},\ x_k \notin \Xi\right)\\ &= \mathbb{P}\left(\forall k \in \{a_1,\ldots,a_{n-1}\},\ x_k \notin \Xi\right)\\ &\quad\times \mathbb{P}\left(x_{a_n} \notin \Xi \mid \Phi \cap \mathcal{C}_{x_{a_1}} = \emptyset, \ldots, \Phi \cap \mathcal{C}_{x_{a_{n-1}}} = \emptyset\right)\\ &= \mathbb{P}\left(\forall k \in \{a_1,\ldots,a_{n-1}\},\ x_k \notin \Xi\right)\\ &\quad\times \exp\left(-(\ell\otimes(\lambda\mu))\left(\mathcal{C}_{x_{a_n}} \cap (\mathcal{C}_{x_{a_1}} \cup \cdots \cup \mathcal{C}_{x_{a_{n-1}}})^c\right)\right)\\ &= \mathbb{P}\left(\forall k \in \{a_1,\ldots,a_{n-1}\},\ x_k \notin \Xi\right)\\ &\quad\times \exp\left(-\lambda\int_0^\infty \ell\left(\mathcal{B}_{x_{a_n}}(r) \cap \mathcal{B}_{x_{a_1}}(r)^c \cap \cdots\right.\right.\\ &\qquad\left.\left.\cap\, \mathcal{B}_{x_{a_{n-1}}}(r)^c\right)\mu(\mathrm{d}r)\right).\end{aligned}$$

From the assumption that the n nodes are aligned, we have

$$\mathcal{B}_{x_{a_n}}(r) \cap \mathcal{B}_{x_{a_1}}(r)^c \cap \ldots \cap \mathcal{B}_{x_{a_{n-1}}}(r)^c = \mathcal{B}_{x_{a_n}}(r) \cap \mathcal{B}_{x_{a_{n-1}}}(r)^c.$$

Thus, in a similar manner to Theorem 1, the volume can be computed as

$$\ell\left(\mathcal{B}_{x_{a_n}}(r) \cap \mathcal{B}_{x_{a_{n-1}}}(r)^c\right) = v_d r^d\left(1 - I_{1-\frac{l^2_{a_n,a_{n-1}}}{4r^2}}\left(\frac{d+1}{2},\frac{1}{2}\right)\right).$$

This concludes the proof. ∎

In multi-hop networks, P_T in (6) becomes

$$\begin{aligned}P_T &= \mathbb{P}\left(\forall k \in \{1,\ldots,n-1\}, \frac{Ph_k l_{k+1,k}^{-\alpha}}{\sigma^2} \geq \gamma_{th}\right)\\ &= \exp\left(-\frac{\tau\sigma^2\gamma_{th}}{P}\sum_{k=1}^{n-1} l_{k+1,k}^\alpha\right).\end{aligned} \tag{14}$$

We may then derive the transmission success probability P_S in (4) using Theorem 2, i.e., (13) and (14).

C. Distribution of the radius

In this subsection, we consider some specific distributions for the radius, i.e., discrete distribution, continuous uniform distribution and Gamma distribution. Then, we introduce more simplified expressions for the integrals in the coverage probability. For the simplicity of presentation, we assume $d = 2$ and define the two integrals appearing in Corollary 1 as

$$\eta_1 \triangleq \int_0^\infty r^2 \, \mu(\mathrm{d}r),$$
$$\eta_2 \triangleq \int_{l/2}^\infty \left(\arccos\left(\frac{l}{2r}\right) - \frac{l}{2r}\sqrt{1-\frac{l^2}{4r^2}} \right) r^2 \, \mu(\mathrm{d}r),$$

so that

$$P_H = 1 - 2\exp\left(-\lambda\pi\eta_1\right) + \exp\left(-2\lambda\pi\eta_1 + 2\lambda\eta_2\right).$$

1) First, assume that the radius can take only a finite number of values, denoted by $R_1, \ldots, R_m \in (0, \infty)$ for some $m \geq 1$, and set $p_i = \mu(\{R_i\})$ for $i = 1, \ldots, m$, which is the probability that the radius is equal to R_i. This corresponds to the following choice of μ

$$\mu(\mathrm{d}r) = \sum_{i=1}^m p_i \, \delta_{R_i}(\mathrm{d}r),$$

where δ_r denotes the Dirac measure at point $r \in [0, \infty)$. Then, we obtain $\eta_1 = \sum_{i=1}^m p_i R_i^2$ and

$$\eta_2 = \sum_{i=1}^m p_i \mathbb{1}_{\{R_i \geq l/2\}} \times \left(\arccos\left(\frac{l}{2R_i}\right) - \frac{l}{2R_i}\sqrt{1-\frac{l^2}{4R_i^2}} \right) R_i^2.$$

2) Next, let us consider the case where the radius is uniformly distributed on $[0, R]$ for a fixed $R \in [0, \infty)$, i.e.,

$$\mu(\mathrm{d}r) = \frac{1}{R}\mathbb{1}_{[0,R]} \, \mathrm{d}r.$$

Then, η_1 can be easily obtained as $\eta_1 = R^2/3$. Now, we focus on the computation of η_2 for $R \geq l/2$ as $\eta_2 = 0$ for $R < l/2$. Note that an antiderivative of $r \mapsto r^2(\arccos(l/(2r)) - l/(2r)\sqrt{1 - l^2/(4r^2)})$ is

$$\varphi(r) \triangleq \frac{r^3}{3}\arccos\left(\frac{l}{2r}\right) - \frac{r^2 l}{3}\sqrt{1-\frac{l^2}{4r^2}} + \frac{l^3}{24}\ln\left(2r\left(1+\sqrt{1-\frac{l^2}{4r^2}}\right)\right).$$

Hence, we can compute η_2 as

$$\eta_2 = \frac{1}{R}\left(\varphi(R) - \varphi\left(\frac{l}{2}\right)\right).$$

3) Last, assume that the radius is Gamma distributed, i.e.,

$$\mu(\mathrm{d}r) = \frac{1}{\Gamma(m)\theta^m} r^{m-1} \mathrm{e}^{-r/\theta} \, \mathrm{d}r,$$

where $m > 0$ and $\theta > 0$ stand for the shape and scale parameters, respectively. Then, we can readily calculate η_1 as

$$\eta_1 = \theta^2 m(1+m).$$

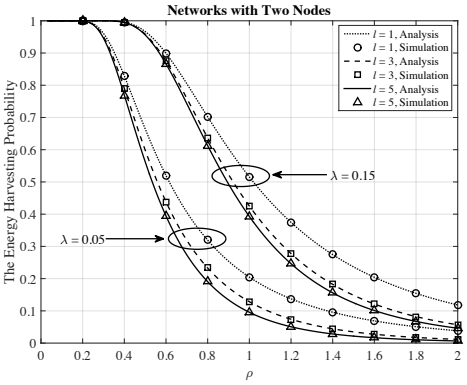

Fig. 6: Comparison of the energy harvesting probability for the networks with two nodes and exponentially distributed radius

We remark that to the best of our knowledge, when the radius is Gamma distributed, the integral η_2 does not have a closed form in terms of standard mathematical functions.

V. Simulation Results

In this section, we provide numerical results to validate our analytical results. We assume that $d = 2$ and use the lines and symbols to denote the analytical and simulated results, respectively. Figs. 6 and 7 illustrate the energy harvesting probability of the networks when the radius is exponentially distributed with parameter ρ, i.e., ρ is an inverse of the mean. Note that this distribution is same as the Gamma distribution with parameters $m = 1$ and $\theta = 1/\rho$. In Fig. 7, the density λ is fixed as $\lambda = 0.15$. From the figures, it is shown that the analytical results match well with the simulated results. Since the mean of the radius decreases as ρ grows, the energy harvesting probability decreases when ρ increases. When the nodes in the network are close together, the probability that the nodes are in the coverage region becomes high. Therefore, in Fig. 6, we can see that the energy harvesting probability increases as the distance between two nodes l becomes small. Also, in Fig. 7, it is shown that the energy harvesting probability decays as the number of sensor nodes increases.

In Figs. 8 and 9, we evaluate the transmission success probability of the networks where the radius is uniformly distributed on $[0, R]$. Here, the SNR is defined as P/σ^2, and $\gamma_{th} = 1$, $\tau = 1$ and $\alpha = 4$. In Fig. 8, the distance between nodes l is set to $l = 2$, and in Fig. 9, the density λ is fixed as $\lambda = 0.15$. We can see that the transmission success probability increases as R grows. This is due to the fact that the coverage region becomes larger as R increases. Moreover, in Fig. 8, it is shown that the transmission success probability grows as the density λ becomes larger. Note that the probability P_T in (6) is the product of the probabilities that the received SNR for each hop is larger than γ_{th}. Consequently, in Fig. 9, we observe that the transmission success probability rapidly decays to zero as the number of hops increases if the SNR is low.

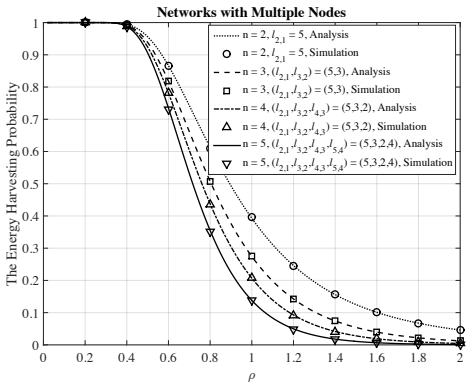

Fig. 7: Comparison of the energy harvesting probability for the networks with multiple nodes and exponentially distributed radius

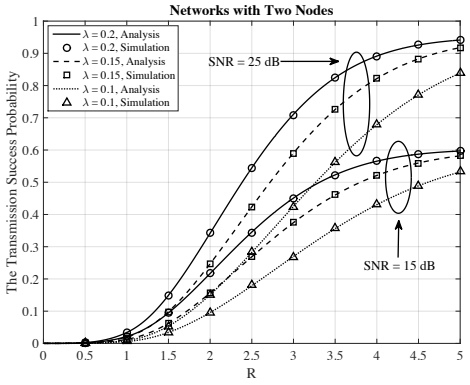

Fig. 8: Comparison of the transmission success probability for the networks with two nodes and uniformly distributed radius

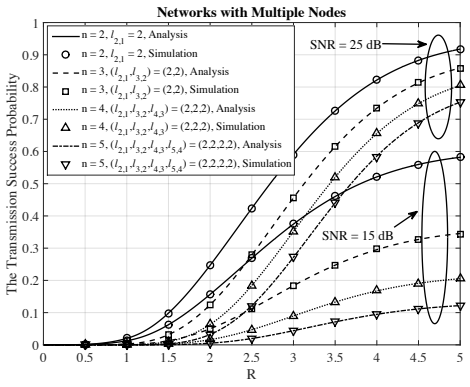

Fig. 9: Comparison of the transmission success probability for the networks with multiple nodes and uniformly distributed radius

VI. Summary

In this paper, we have presented a novel analytical framework for analyzing the performance of wireless energy harvesting networks. The framework is based on the classical Boolean-Poisson model. The probability of a single node being covered by the Boolean-Poisson model is well-known. We have extended this computation by considering the cases of two nodes and multiple nodes. The former involves the transmitter and receiver, while the latter also includes relays. In both of these settings, the energy harvesting probability and transmission success probability have been derived. We have conducted an extensive simulation to validate the described analytical framework.

Acknowledgements

This work was supported in part by the National Research Foundation of Korea (NRF) grant funded by the Korean government (MSIP) (2014R1A5A1011478), Singapore MOE Tier 1 (RG18/13 and RG33/12) and MOE Tier 2 (MOE2014-T2-2-015 ARC 4/15 and MOE2012-T2-2-033 ARC 3/13).

References

[1] X. Lu, P. Wang, D. Niyato, D. I. Kim, and Z. Han, "Wireless Networks With RF Energy Harvesting: A Contemporary Survey," *IEEE Commun. Surv. Tut.*, vol. 17, pp. 757–789, Second Quarter 2015.

[2] R. Zhang and C. K. Ho, "MIMO Broadcasting for Simultaneous Wireless Information and Power Transfer," *IEEE Trans. Wireless Commun.*, vol. 12, pp. 1989–2001, May 2013.

[3] J. Park and B. Clerckx, "Joint Wireless Information and Energy Transfer in a K-User MIMO Interference Channel," *IEEE Trans. Wireless Commun.*, vol. 13, pp. 5781–5796, Oct. 2014.

[4] H. Lee, S.-R. Lee, K.-J. Lee, H.-B. Kong, and I. Lee, "Optimal Beamforming Designs for Wireless Information and Power Transfer in MISO Interference Channels," *IEEE Trans. Wireless Commun.*, vol. 9, pp. 4810–4821, Sep. 2015.

[5] K. Huang and V. K. N. Lau, "Enabling Wireless Power Transfer in Cellular Networks: Architecture, Modeling and Deployment," *IEEE Trans. Wireless Commun.*, vol. 13, pp. 902–912, Feb. 2014.

[6] J. Guo, S. Durrani, X. Zhou, and H. Yanikomeroglu, "Outage Probability of Ad Hoc Networks With Wireless Information and Power Transfer," *IEEE Commun. Lett.*, vol. 4, pp. 409–412, Aug. 2015.

[7] A. H. Sakr and E. Hossain, "Analysis of K-Tier Uplink Cellular Networks With Ambient RF Energy Harvesting," *IEEE J. Sel. Areas Commun.*, vol. 33, pp. 2226–2238, Oct. 2015.

[8] S. N. Chiu, D. Stoyan, W. S. Kendall, and J. Mecke, *Stochastic Geometry and Its Applications*. Third Edition, Wiley, 2013.

[9] R. Meester and R. Roy, *Continuum Percolation*. Cambridge University Press, 1996.

[10] P. Hall, "On Continuum Percolation," *Ann. Probab.*, vol. 13, pp. 1250–1266, 1985.

[11] P. Hall, "On the Coverage of k-Dimensional Space by k-Dimensional Spheres," *Ann. Probab.*, vol. 13, pp. 991–1002, 1985.

[12] H. Biermé and A. Estrade, "Covering the Whole Space With Poisson Random Balls," *ALEA Lat. Am. J. Probab. Math. Stat.*, vol. 9, pp. 213–229, 2012.

[13] J. Serra, *Image Analysis and Mathematical Morphology*. Academic Press, 1984.

[14] F. Baccelli, Bartłomiej, and Błaszczyszyn, "On a Coverage Process Ranging from the Boolean Model to the Poisson Voronoi Tessellation With Applications to Wireless Communications," *Adv. in Appl. Probab.*, vol. 33, pp. 293–323, 2001.

[15] M. Haenggi, J. G. Andrews, F. Baccelli, O. Dousse, and M. Franceschetti, "Stochastic Geometry and Random Graphs for the Analysis and Design of Wireless Networks," *IEEE J. Sel. Areas Commun.*, vol. 27, pp. 1029–1046, Sep. 2009.

[16] S. Li, "Concise Formulas for the Area and Volume of a Hyperspherical Cap," *Asian J. Math. Stat.*, vol. 4, pp. 66–70, 2011.